







Article

Experimental and Computational Analysis of Newly Synthesized Benzotriazinone Sulfonamides as Alpha-Glucosidase Inhibitors

Zunera Khalid ¹, Maha Abdallah Alnuwaiser ² , Hafiz Adnan Ahmad ³ , Syed Salman Shafqat ^{4,*} ,
Munawar Ali Munawar ^{3,5}, Kashif Kamran ⁶, Muhammad Mujtaba Abbas ⁷ , M. A. Kalam ⁸ 
and Menna A. Ewida ⁹ 

¹ Department of Chemistry, Kinnaird College for Women, Lahore 54000, Pakistan

² Department of Chemistry, College of Science, Princess Nourah bint Abdulrahman University, P.O. Box 84428, Riyadh 11671, Saudi Arabia

³ School of Chemistry, University of the Punjab, Lahore 54590, Pakistan

⁴ Department of Chemistry, Division of Science and Technology, University of Education, Lahore 54770, Pakistan

⁵ Department of Basic and Applied Chemistry, FAST, University of Central Punjab, Lahore 54000, Pakistan

⁶ Department of Physics, University of Agriculture, Faisalabad 38040, Pakistan

⁷ Department of Mechanical Engineering, University of Engineering and Technology (New Campus), Lahore 54890, Pakistan

⁸ Faculty of Engineering and IT, University of Technology, Sydney 2007, Australia

⁹ Department of Pharmaceutical Chemistry, Faculty of Pharmacy, Future University in Egypt, New Cairo 11835, Egypt

* Correspondence: salman.shafqat@ue.edu.pk; Tel.: +92-331-413-9585



Citation: Khalid, Z.; Alnuwaiser, M.A.; Ahmad, H.A.; Shafqat, S.S.; Munawar, M.A.; Kamran, K.; Abbas, M.M.; Kalam, M.A.; Ewida, M.A. Experimental and Computational Analysis of Newly Synthesized Benzotriazinone Sulfonamides as Alpha-Glucosidase Inhibitors. *Molecules* **2022**, *27*, 6783. <https://doi.org/10.3390/molecules27206783>

Academic Editors: Philippe Belmont, Wim Dehaen and Eugene Babaev

Received: 31 August 2022

Accepted: 21 September 2022

Published: 11 October 2022

Publisher's Note: MDPI stays neutral with regard to jurisdictional claims in published maps and institutional affiliations.



Copyright: © 2022 by the authors. Licensee MDPI, Basel, Switzerland. This article is an open access article distributed under the terms and conditions of the Creative Commons Attribution (CC BY) license (<https://creativecommons.org/licenses/by/4.0/>).

Abstract: Diabetes mellitus is a chronic metabolic disorder in which the pancreas secretes insulin but the body cells do not recognize it. As a result, carbohydrate metabolism causes hyperglycemia, which may be fatal for various organs. This disease is increasing day by day and it is prevalent among people of all ages, including young adults and children. Acarbose and miglitol are famous alpha-glucosidase inhibitors but they complicate patients with the problems of flatulence, pain, bloating, diarrhea, and loss of appetite. To overcome these challenges, it is crucial to discover new anti-diabetic drugs with minimal side effects. For this purpose, benzotriazinone sulfonamides were synthesized and their structures were characterized by FT-IR, ¹H-NMR and ¹³C-NMR spectroscopy. *In vitro* alpha-glucosidase inhibition studies of all synthesized hybrids were conducted using the spectrophotometric method. The synthesized compounds revealed moderate-to-good inhibition activity; in particular, nitro derivatives **12e** and **12f** were found to be the most effective inhibitors against this enzyme, with IC₅₀ values of 32.37 ± 0.15 μM and 37.75 ± 0.11 μM. *In silico* studies, including molecular docking as well as DFT analysis, also strengthened the experimental findings. Both leading compounds **12e** and **12f** showed strong hydrogen bonding interactions within the enzyme cavity. DFT studies also reinforced the strong binding interactions of these derivatives with biological molecules due to their lowest chemical hardness values and lowest orbital energy gap values.

Keywords: 1,2,3-Benzotriazin-4(3H)-one; molecular docking studies; alpha-Glucosidase inhibitors

1. Introduction

Diabetes mellitus is a metabolic disorder of the endocrine system characterized by hyperglycemia due to impaired insulin tolerance [1,2]. Insulin is the peptide hormone that maintains glucose homeostasis; it binds to cell receptors for the transfer of glucose molecules. This hormone also stimulates fat cells and muscles to obtain glucose from the blood and accelerates the liver for glucose metabolism until the sugar level is lowered

to normal [3]. In diabetes mellitus, the pancreas prepares insulin but body cells do not recognize it. As a result, food intake causes hyperglycemia and body cells suffer glucose deficiency [4]. Early symptoms of diabetes are excessive thirst, nausea, shortness of breath, fatigue and frequent urination, but unattended prolonged hyperglycemia can cause other aberrations, including leg amputation, blindness, nerve damage, kidney failure and cardiovascular complications [1,5].

In early times, this disease was known as adult-onset diabetes, but by the end of the twentieth century, it was being widely diagnosed among teens and the pediatric age group. The worldwide prevalence of diabetes among children and young adults is an alarming situation [6]. Diabetes mellitus may be inherent, however, other factors such as smoking, sedentariness, obesity, inactivity and fast food consumption are major causes of this disease [7]. According to the International Diabetes Federation, 536.6 million people were reported to have diabetes in 2021 and this number will increase to 783.2 million by 2045 [8]. Once a patient develops diabetes, that patient suffers from it for the rest of their life [9]. Exercise, weight control and good eating habits can reduce the risk of occurrence.

In the intestines, alpha-glucosidase is an enzyme that converts food polysaccharides into absorbable glucose, which then enters the blood and increases sugar level [10–12]. Therefore, inhibition of alpha-glucosidase is an effective strategy to control hyperglycemia [13]. Commercially, acarbose (Glucobay) and miglitol (Glyset) are famous alpha-glucosidase inhibitors, but daily consumers of these drugs complain of bloating, diarrhea and flatulence, leading to loss of appetite [14–18]. To overcome these side effects, it is crucial to explore new alpha-glucosidase inhibitors with better inhibition potency and minimal side effects.

Sulfonamide is a famous pharmacophore responsible for several biological activities; it is a part of many clinical drugs [19,20]. Different heterocyclic groups with sulfonamide functionality have been studied as alpha-glucosidase inhibitors. Coumarin sulfonamide **1** [21], chromone sulfonyl hydrazone **2** [21], indole sulfonyl hydrazide **3** [22] and indole sulfonamide **4** [23] have been reported to be strong alpha glucosidase inhibitors (Figure 1). 1,2,3-Benzotriazin-4(3H)-one is known for its biologically active nucleus, and its derivatives have been reported as anti-inflammatory [24], anti-depressant [25], anticancer [26], anti-diarrheal [27], HIV inhibitor [28] and as anesthetics [29]. Some of its derivatives had been studied as enzyme inhibitors of 4-hydroxyphenylpyruvate dioxygenase [30], matrix metalloprotease [31], alpha-glucosidase [15], chorismate mutase [32], HepG2 [33] and acetylcholinesterase [34].

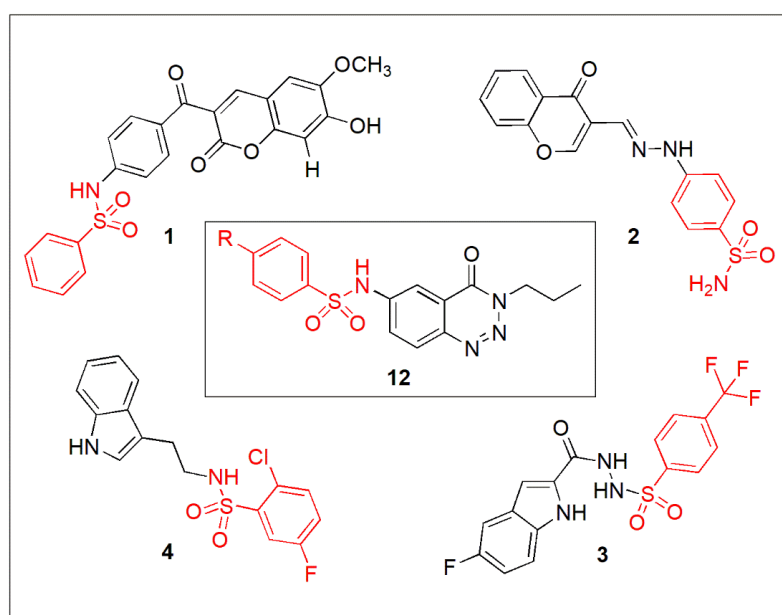


Figure 1. Reported structures of heterocyclic sulfonamides as alpha-glucosidase inhibitors.

In our efforts to develop an anti-diabetic drug with an enhanced therapeutic effect, we reported a series of benzotriazinone sulfonamide derivatives as potent alpha-glucosidase inhibitors, and one of them, compound **4** (Figure 2), exhibited good results, with an IC_{50} value of $29.75 \pm 0.14 \mu\text{M}$ [15]. In order to further enhance the potency of compound **4**, our group designed another series of benzotriazinone sulfonamide derivatives (**12a–f**). This design mainly involved the replacement of the aryl group of compound **4** by alkyl moiety at the third position, as well as the introduction of sulfonamide moiety at the sixth position of benzotriazinone (Figure 2). Novel hybrids of 4-phenyl-*N*-(4-oxo-3-alkyl-3,4-dihydrobenzo[1,2,3]triazin-6-yl)benzenesulfonamide (**12a–f**) were prepared and their *in vitro* inhibition potential was studied in comparison to the commercial drug acarbose. Moreover, molecular docking analysis was employed to explain *in vitro* studies and to explore the binding mode of interactions of all hybrids against the binding sites of target alpha glucosidase. Furthermore, the stability and reactivity of the screened compounds were calculated by DFT studies to explore their hybrid interactions with other molecules.

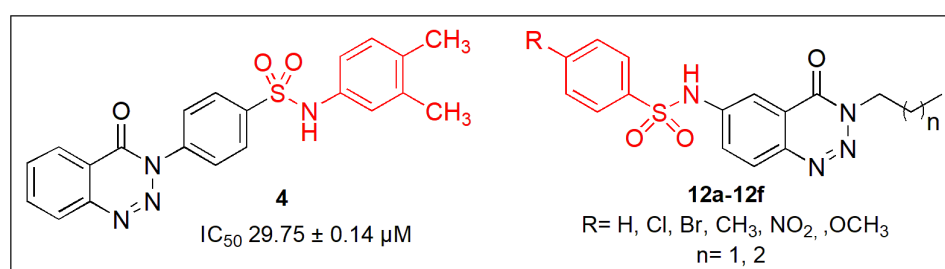


Figure 2. Design of new 1,2,3-benzotriazin-4(3H)-one sulfonamides **12a–12f**.

2. Results and Discussion

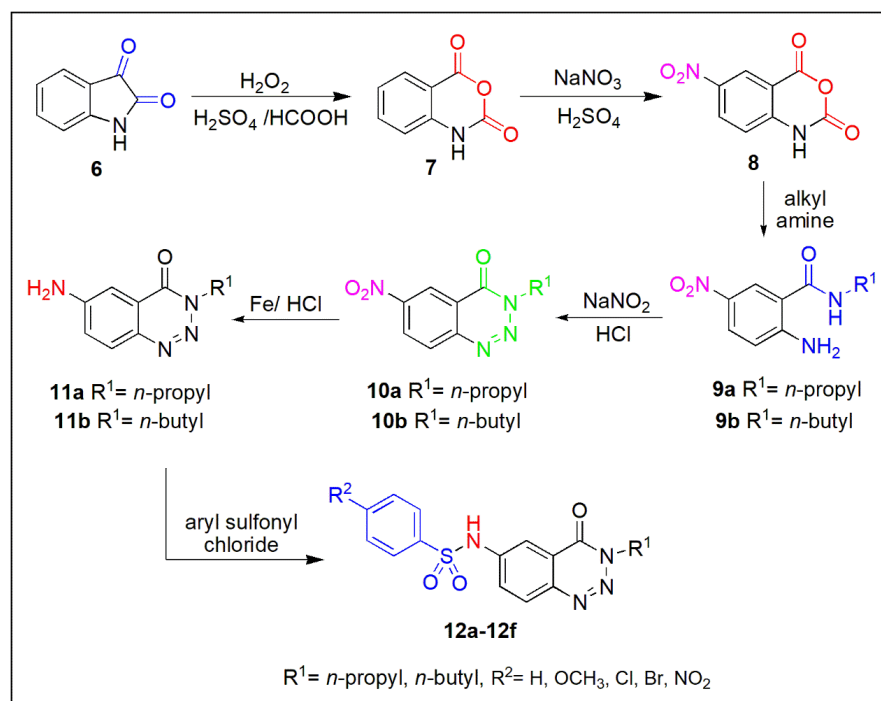
2.1. Synthetic Chemistry

1,2,3-Benzotriazin-4(3H)-one-based sulfonamides (**12a–12f**) were synthesized by using isatin (**6**) as an inexpensive starting material; it was initially oxidized to isatoic anhydride (**7**) and then nitrated in a sodium nitrate/sulfuric acid mixture to prepare 6-nitroisatoic anhydride (**8**) followed by reaction with *n*-propyl and *n*-butylamine to prepare their corresponding anthranilamides (**9a**, **9b**, Scheme 1). Further cyclization was conducted in a nitrous acid mixture to yield **10a** and **10b** followed by reduction with Fe/HCl mixture. In the final step, 6-amino-*N*-propyl-1,2,3-benzotriazin-4(3H)-one (**11a**) and 6-amino-*N*-butyl-1,2,3-benzotriazin-4(3H)-one (**11b**) were reacted with different arylsulfonyl chlorides to accomplish various sulfonamide hybrids **12a–12f** (Scheme 1).

2.2. Spectroscopic Characterization

In multistep synthesis, the starting compounds **7**, **8**, **9a**, **9b**, **10a** and **10b** were prepared and characterized by FTIR spectral analysis, and observations were consistent with the values of similar compounds found in the literature [35,36]. The FTIR spectrum of isatoic anhydride **7** displayed strong absorption bands at $1722, 1765 \text{ cm}^{-1}$ (C=O) and 1021 cm^{-1} (C–O–C), indicating the presence of anhydride moiety [35]. Regarding nitration, the presence of the NO_2 group in compound **8** was identified by FTIR band at 1355 cm^{-1} [36]. The anhydride group of compound **8** was reacted with alkyl amines, and as a result, *N*-alkyl anthranilamides **9a** and **9b** were formed as products, which were confirmed by the appearance of amino group IR bands at $3293\text{--}3318 \text{ cm}^{-1}$ [37]. Further cyclization of anthranilamides was confirmed by the disappearance of NH_2 bands in both nitro benzotriazinones **10a** and **10b** [38]. Reduction of the NO_2 group to NH_2 was confirmed by the appearance of an IR band at 3430 cm^{-1} [39]. In sulfonamides (**12a–12f**), symmetrical stretching vibrational bands of S=O and NH were observed at $1157\text{--}1187$ and $3185\text{--}3221 \text{ cm}^{-1}$ [15]. Amino products **11a** and **11b** and all final products (**12a–12f**) were further characterized by $^1\text{H-NMR}$ and $^{13}\text{C-NMR}$ spectroscopic techniques. The amino group of **11a** and **11b** appeared at 6.56 ppm, while after conversion into the sulfonamide group, the NH group was noted to

be in the range of 11.35–11.47 ppm. $^1\text{H-NMR}$ analysis of **11a**, **11b** and **12a–12f** revealed the propyl protons as triplet, multiplet and triplet in the range of 0.84–4.82 ppm and the aromatic protons of phenyl rings were observed in the range of 7.02–8.12 ppm. Further $^{13}\text{C-NMR}$ spectral results confirmed the structure of all synthesized compounds.



Scheme 1. Synthetic route for the synthesis of 1,2,3-benzotriazin-4(3H)-one based sulfonamides.

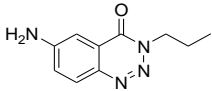
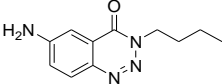
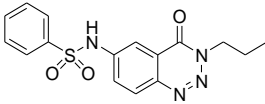
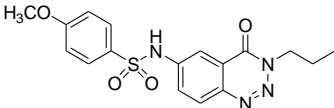
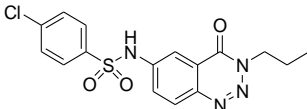
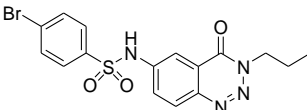
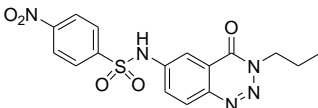
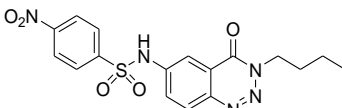
2.3. Alpha-Glucosidase Inhibition Studies

Acarbose is a commercially available antidiabetic drug used to treat diabetes mellitus. It actively works in the intestinal tract by inhibiting alpha-glucosidase, which is responsible for the conversion of complex carbohydrates to absorbable glucose. Acarbose has various side effects and chemists are working to discover a new effective anti-diabetic drug. Therefore, an alpha-glucosidase inhibition assay of newly synthesized amino benzotriazinones **11a–11b** and their corresponding sulfonamides **12a–12f** was carried out by spectrophotometric method. Comparative results of all compounds (**12a–12f**) with reference to standard drug acarbose are given in Table 1. The results proved to have fair to good inhibition activity. From Table 1, it is evident that amino benzotriazinones **11a** and **11b** exhibited less inhibition in contrast to their sulfonamides, which indicated the effective interactions of sulfonyl group within the enzyme cavity. Nitro derivative **12e** revealed the most promising activity, with an IC_{50} value of $32.37 \pm 0.15 \mu\text{M}$ as compared to the standard drug acarbose, with an IC_{50} value of $37.38 \pm 0.12 \mu\text{M}$. Another nitro compound (**12f**) with the butyl group was found to be an equivalent inhibitor of acarbose, with an IC_{50} value of $37.75 \pm 0.11 \mu\text{M}$.

The difference in the inhibition potentials of **12e** and **12f** illustrated that the small chain of the propyl group is more appropriate to be fitted with an alpha-glucosidase structure. Electron density on oxygen atoms of the nitro group enabled it to have a strong inhibitory potential. Different groups at the fourth position of the phenyl ring revealed different inhibition strengths. Compound **12a** indicated a lesser enzyme inhibition potency as compared to other compounds having Cl, Br, NO_2 and OCH_3 groups. The lone pair containing substituents on the phenyl ring supported inhibition activity due to their electronic interactions with enzyme (active) sites. The larger size of the bromine atom reduced the inhibition activity of compound **12d** (IC_{50} value $55.21 \pm 0.12 \mu\text{M}$) as compared to the chloro-containing compound **12c** (IC_{50} value $53.27 \pm 0.13 \mu\text{M}$). The

methoxy derivative **12b** was found to be more effective inhibitor as compared to **12a** but less active than **12e** and **12f**.

Table 1. Results of alpha-glucosidase inhibition studies.

Sr. No.	Codes	Structures	% Inhibition at 0.5 mM	IC ₅₀ (μM)
1.	11a		26.12 ± 0.13	ND
2.	11b		27.12 ± 0.13	ND
3.	12a		51.25 ± 0.16	<500
4.	12b		91.73 ± 0.17	39.21 ± 0.12
5.	12c		78.12 ± 0.16	53.76 ± 0.14
6.	12d		79.42 ± 0.15	55.21 ± 0.12
7.	12e		96.27 ± 0.19	32.37 ± 0.15
8.	12f		93.27 ± 0.14	37.75 ± 0.11
9.	Standard	acarbose	92.23 ± 0.16	37.38 ± 0.12

2.4. Molecular Docking

The probable binding interactions of the tested compounds within the enzyme cavity were explored by molecular docking studies. Autodoc Vina and its tools were utilized to elaborate all types of interactions. The receptor file of alpha-glucosidase was prepared by homology modeling, as reported in our previous work [15]. Chemdraw office pack was utilized to prepare and optimize the ligand's structure by using the MM2 force field.

Both **12e** and **12f** formed stable ligand enzyme complexes and displayed the highest binding energy, -9.5 and -9.3 kcal.mol⁻¹, respectively. Binding pose of the docked conformation with highest binding affinity of both ligands **12e** and **12f** are presented in Figures 3 and 4, respectively. From these figures, it is evident that both ligands are fit inside the enzyme pockets due to different kinds of binding interactions, including electrostatic, hydrogen bonding as well as hydrophobic interactions. In these two cases, the highest binding may be associated with the development of hydrogen bonding between the carbonyl group of ligands and the carboxylic group of GLU276. The nitro group of **12e** and **12f** also established hydrogen bonding with the NH group of HIS279. Similarly, one conventional hydrogen bond can be seen between nitrogen of the benzotriazinone ring and the NH group of the ARG439 amino acid (Figures 3 and 4).

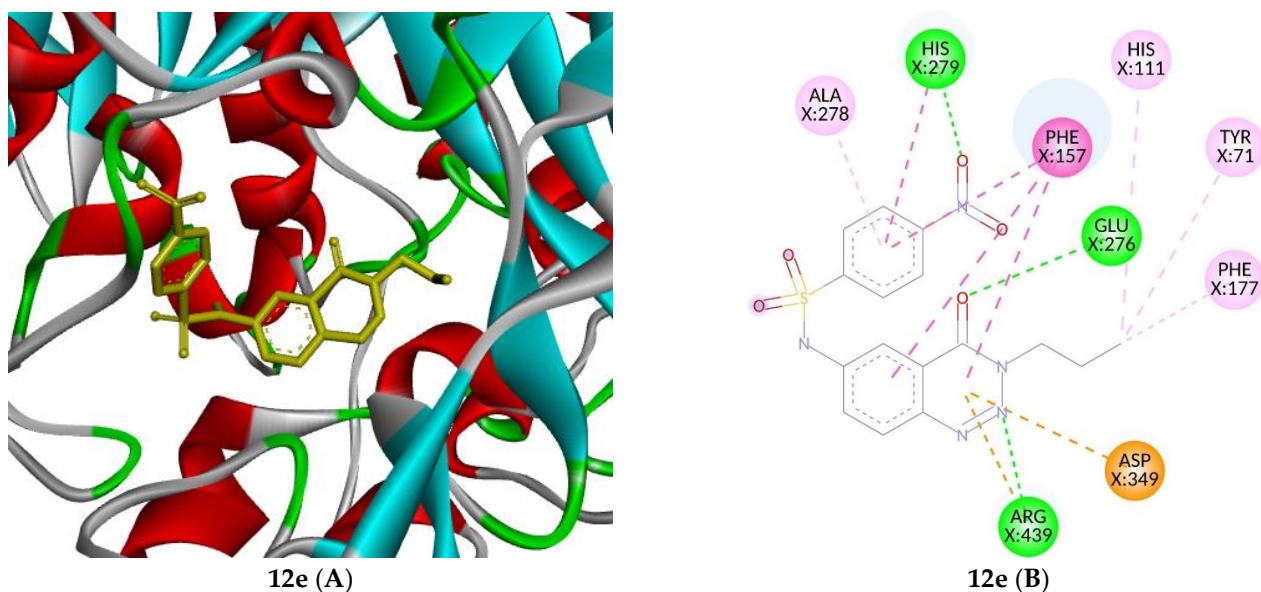


Figure 3. 2D (B) and 3D (A) structures illustrating docking results, ligand **12e** within alpha-glucosidase develops the interactions shown by colored lines; hydrogen bonding (green), pi-cationic/pi anionic interaction (brown), pi-pi interaction (pink) and pi-alkyl interaction (purple).

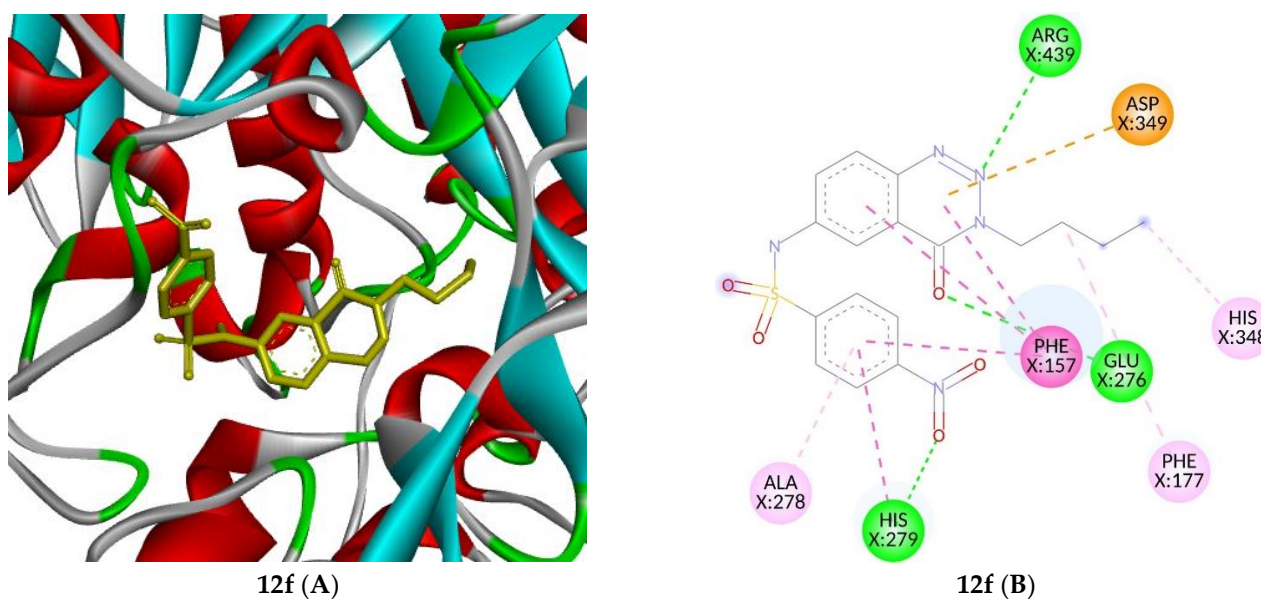


Figure 4. 2D (B) and 3D (A) structures illustrating docking results, ligand **12f** within alpha-glucosidase develops interactions shown by colored lines; hydrogen bonding (green), pi-cationic/pi anionic interaction (brown), pi-pi interaction (pink) and pi-alkyl interaction (purple).

Similarly, the benzotriazinone ring of both ligands (**12e** and **12f**) depicted pi-anionic electrostatic interaction with the carboxylic acid group of ASP349. However, an additional pi-cationic interaction between the NH group of ARG349 and the benzotriazinone ring was found in the case of compound **12e** (Figures 3 and 4).

All rings, along with alkyl groups of both ligands **12e** and **12f**, established various kinds of hydrophobic interactions with the residues of different amino acids (Figures 3 and 4). Significantly, pi-pi T-shaped interactions appeared between pi-electron densities of both ligands and aromatic side chains of PHE157 and HIS279. Similarly, pi-alkyl interactions between the methyl group of ALA278 and the ring density of the benzene ring attached with the nitro group can be observed in the case of both ligands. All mentioned forces made strong

ligand enzyme complexes that enabled these compounds (**12e** and **12f**) to act as effective alpha-glucosidase inhibitors. Molecular docking results explored that both **12e** and **12f** docked compounds have almost similar kinds of interactions within the active pockets of enzyme (Figures 3 and 4). However, the relatively lesser activity of compound **12f** as compared to **12e** can be explained in terms of increasing hydrophobicity of the ligand due to the increasing chain of the alkyl group in compound **12f** that makes the ligand–enzyme complex relatively less stable, as observed in the binding energies.

2.5. Computational Study

2.5.1. Frontier Molecular Orbital Analysis

Quantum chemistry calculations regarding the highest occupied molecular orbital (HOMO) and lowest unoccupied molecular orbital (LUMO) are collectively known as frontier molecular orbital analyses (FMO). FMO analyses are helpful in drug design and in determining reactivity. HOMO is the highest energy orbital of molecule with electrons while LUMO is the lowest energy orbital of molecule with no electrons [40]. Energy difference between HOMO and LUMO is the main factor for compound reactivity. All synthesized compounds **12a–12f** were studied by frontier molecular orbital analysis and results supported that all synthesized molecules have high chemical reactivity [41,42].

Energy of HOMO (E_{HOMO}), LUMO (E_{LUMO}) and energy gaps ($E_{\text{gap}} = \text{HOMO} - \text{LUMO}$) between them were calculated by B3LYP/6-311+G* level of DFT method (Table 2). Large energy gap value illustrates that compound is less reactive while small energy gap indicates the less kinetic stability and high chemical reactivity. Among all compounds, **12e** and **12f** were found to have lowest energy gap values revealing that these compounds are more reactive as compared to others. Furthermore, the HOMO-LUMO energy analysis of all compounds provided valuable information about their global reactivity descriptors like E_{HOMO} , E_{LUMO} , electrophilicity, chemical potential, chemical softness and various other electronic parameters which are tabulated in Table 2 [40,43].

Table 2. Electronic parameters of synthesized compounds (**12a–f**).

Compounds	E_{HOMO}	E_{LUMO}	E_{gap}	I	A	η	S	μ	X	ω	D
12a	−6.62	−2.06	4.55	6.62	2.06	2.28	0.22	4.34	4.34	4.14	5.54
12b	−6.52	−1.98	4.54	6.52	1.98	2.27	0.22	4.25	4.25	3.98	7.07
12c	−6.73	−2.17	4.56	6.73	2.17	2.28	0.22	4.45	4.45	4.34	3.67
12d	−6.70	−2.15	4.55	6.70	2.15	2.27	0.22	4.43	4.43	4.31	3.89
12e	−7.02	−3.33	3.70	7.02	3.33	1.85	0.27	5.18	5.18	7.25	2.30
12f	−7.01	−3.33	3.68	7.01	3.33	1.84	0.27	5.17	5.17	7.26	2.35

The electrophilicity values (ω) of all compounds explained their bonding, stability, structure and reactivity [40,43]. Compounds **12e** and **12f** presented the highest values of electrophilicity, 7.25 and 7.26 eV, which is evidence of their greater interactions with biomolecules. Electrophilicity index with molecular docking studies supported the in vitro alpha-glucosidase inhibition results where **12e** and **12f** exhibited good inhibitory activity.

For the synthesized series **12a–12f**, delocalization of both HOMO and LUMO was identified by charge density, as demonstrated in Figure 5. It was observed that HOMO is located on the site of the benzotriazinone ring, and sulfonamide moiety and LUMO delocalization is different in different molecules. The compound with no substitution, **12a**, as well as the compound with an electron donating group, **12b**, exhibited their LUMO delocalizations confined on the benzotriazinone ring. While in compounds **12c** and **12d**, the electron density of LUMO was delocalized on their phenyl ring and sulfonamide moiety. However, **12a**, **12b** and **12d** have LUMO delocalization on the surface of the benzotriazinone ring and sulfonamide group (Figure 5). The compounds **12c**, **12d**, **12e** and **12f** have electron withdrawing groups (Cl, Br and NO_2), restraining LUMO electron density only on the phenyl ring.

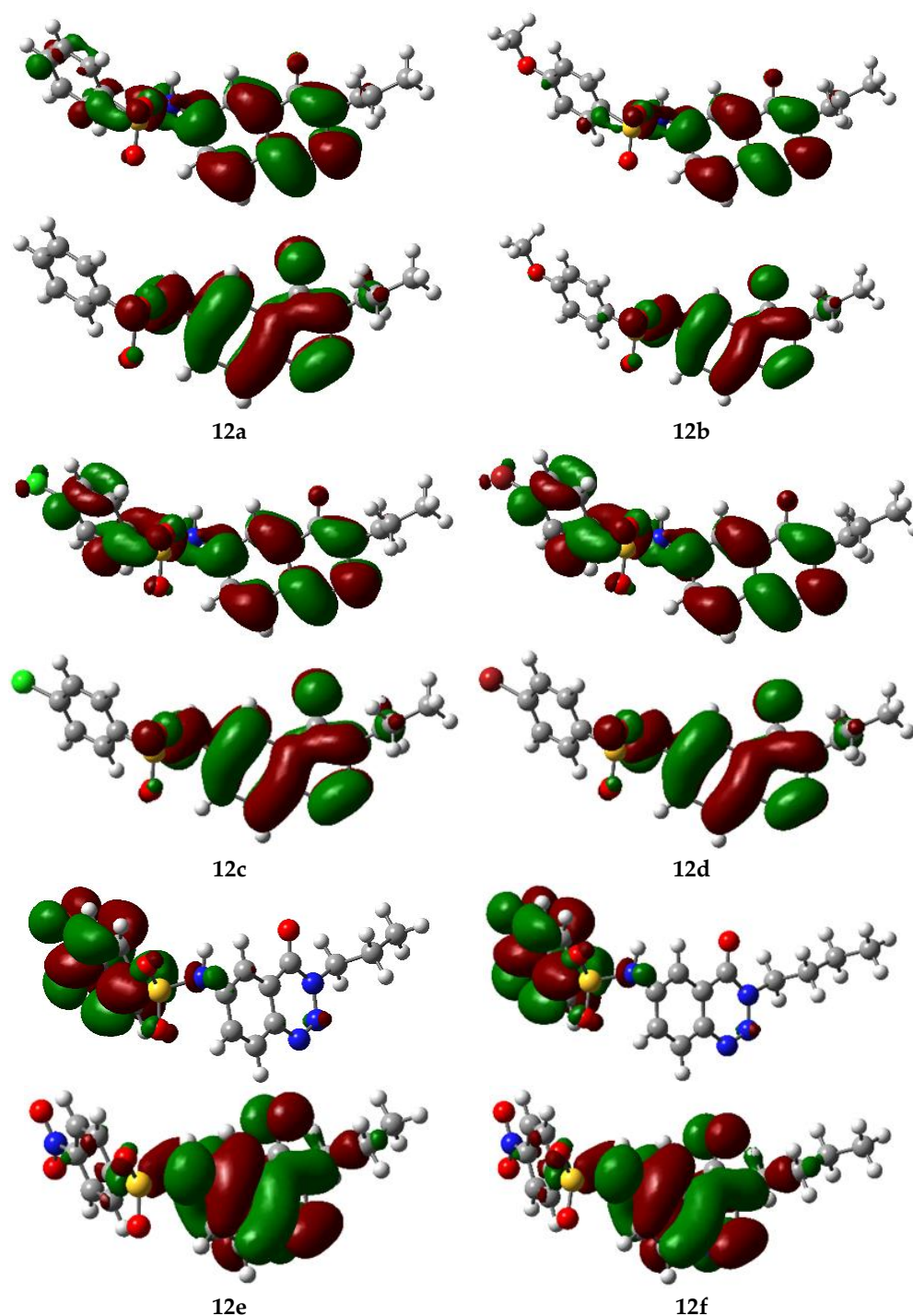


Figure 5. Pictorial illustration of charge density distribution in molecular orbitals of compounds 12a–12f. HOMO is shown at the bottom and LUMO is displayed at the top.

2.5.2. Molecular Electrostatic Potential

At the molecular level, MEP is an effective method to describe the electron density distribution map inside molecules and can illustrate an idea about the reactive sites of molecular structure. This method provides images according to the relative polarity present in a molecule, which indicate the electrophilic portion (negative site) and nucleophilic portion (positive side) of the compound. MEP studies were carried out using a B3LYP/6-311+G* method and the results are shown in Figure 6. Surface maps displayed pictures with different colors, indicating different electrostatic potential values. The positive sites are shown by the

blue colour, while the yellow colour depicts slightly positive areas, and neutral electrostatic potential regions are represented by green. The positive sites indicated by the blue colour of all molecules tend to repel protons. Further, this study helped to identify reactive sites of chemical systems and indicated the sites where ligand can bind to enzyme. MEP analysis of all compounds depicted the existence of strong positive potential on hydrogen atoms of sulfonamide functionality and partial positive charge on C=O, N=N and SO₂ groups. The existence of strong and partial positive charges on functional groups of synthesized series have a tendency to develop appropriate interactions within the enzyme cavity.

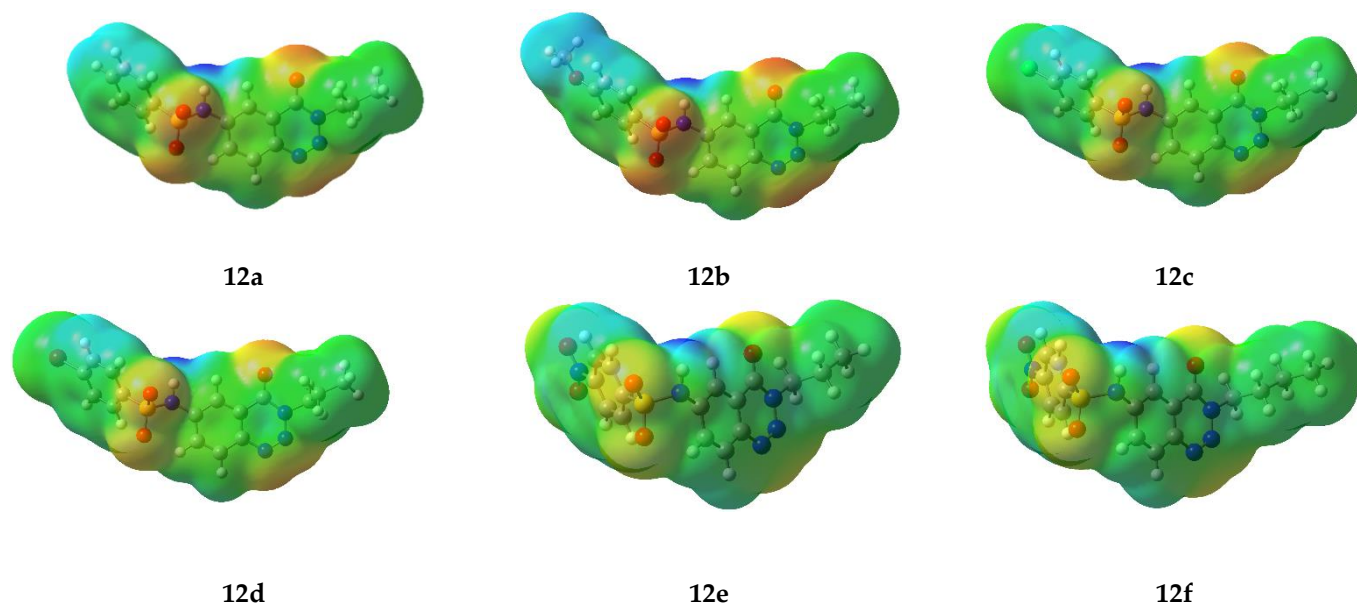


Figure 6. Electrostatic potential on the surfaces of 1,2,3-benzotriazin-4(3H)-one sulfonamides.

3. Experiment Work

3.1. General

All chemicals were purchased from international supplier, Sigma-Aldrich (USA and Germany), Fluka (Switzerland). Merck TLC plates (Germany) were used to monitor the progress of reactions under short and long wavelengths (model UVGL-25 minor light multi-band UV-254/366). VWR formic acid (USA) and Merck glacial acetic acid (Germany) were used in the synthesis of isatoic anhydride. Melting points were recorded on the Fisher–Johns apparatus (University of the Punjab, Lahore), calibrated by benzoic acid. The FTIR spectra were taken on Agilent 630 FTIR (University of the Punjab, Lahore). In NMR (H.E.J Research institute of chemistry, University of Karachi), TMS was used as internal standard and all spectra were recorded in CDCl₃ or DMSO-d₆ on Bruker (300, 400 and 500 MHz).

3.1.1. Synthesis of Isatoic Anhydride (7)

Isatin (**6**, 14.7 g, 0.1 mmol) and formic acid (80 mL) were taken in an Erlenmeyer flask. Hydrogen peroxide (30%, 20 mL) was added slowly with slight cooling, and the reaction mixture was stirred for 1h at room temperature. Precipitates of product appeared in the flask and were filtered and recrystallized from methanol. Light yellow compound; yield: (13.85 g, 85%); m.p. 230–232 °C (Lit. m.p. with decomposition: 235 °C [36]. FT-IR (v-cm⁻¹): 1021 (C-O-C), 1722 (C=O), 1765 (C=O), 3236 (N-H).

3.1.2. 6-Nitroisatoic Anhydride (8)

Isatoic anhydride (**7**, 3.42 g, 21 mmol) and chilled concentrated sulfuric acid (98%, 18.4 M, 75 mL) were taken in a round bottom flask (250 mL). Sodium nitrate (2.22 g, 26.25 mmol) was added in small portions and ice-bath was used to maintain the temperature below 5 °C. Then, the reaction mixture was stirred for 15 min and poured off into ice-cold

water (500 mL). Precipitates formed on slight stirring were filtered, dried and recrystallized from ethanol. Yellow powder; yield: (2.45 g, 62%); m.p. 219–221 °C (Lit. m.p. 220 °C) [44]. FT-IR (ν -cm⁻¹): 1355 (NO₂), 1578 (NO₂), 1680 (C=O), 1738 (C=O), 3198 (N-H).

3.1.3. 2-Amino-5-nitro-N-alkylbenzamides (9a–9b)

6-nitroisatoic anhydride (**8**, 4 g, 19.2 mmol) and alkylamine (19.2 mmol) were mixed in 1,4-dioxan and heated under reflux. After 3h, the solvent was evaporated under reduced pressure and the residue was recrystallized from methanol and further dried at 70 °C.

2-Amino-5-nitro-N-propylbenzamide (9a). Propylamine (1.58 mL, 19.2 mmol) and 6-nitroisatoic anhydride (**8**, 4 g, 19.2 mmol) were used to prepare mustard powder; yield: (2.80 g, 60%); m.p. 195–197 °C. FT-IR (ν -cm⁻¹): 1334 (NO₂), 1522 (NO₂), 1608 (C=O), 3293 (NH₂).

2-Amino-5-nitro-N-butylbenzamide (9b). Butylamine (1.87 mL, 19.2 mmol) and 6-nitroisatoic anhydride (**8**, 4 g, 19.2 mmol) were used to synthesize mustard powder; yield: (2.75 g, 58%); m.p. 197–199 °C. FT-IR(ν -cm⁻¹): 1333 (NO₂), 1536 (NO₂), 1650 (C=O), 3318 (NH₂).

3.1.4. General Procedure for the Synthesis of 6-Nitro-3-alkylbenzo[1,2,3]triazin-4(3H)-ones (10a–10b)

In a conical flask, compound **9a/9b** (3 g, 12.8 mmol) was taken in chilled water (20 mL), and HCl solution (30%, 5 mL) was added into it. The reaction mixture was placed in an ice bath to maintain the temperature at 0–5 °C. Sodium nitrite (16.6 mmol) was dissolved in distilled water (10 mL) and this solution was slowly added to the reaction mixture; the temperature was maintained below 5 °C. Afterwards, the reaction was stirred for two hours and ice-cold water was added to obtain precipitates of product. The product was washed twice with chilled water and recrystallized from methanol followed by drying at 70 °C.

6-Nitro-3-propylbenzo[1,2,3]triazin-4(3H)-one (10a). Compound **9a** (3 g, 12.8 mmol), HCl solution (30%, 5 mL) and sodium nitrite (1.16 g, 16.6 mmol) were used to obtain light yellow powder; yield: (2.80 g, 92%); m.p. 215–217 °C. FT-IR (ν -cm⁻¹): 1344 (NO₂), 1530 (NO₂), 1687 (C=O), 2968 (CH₂).

6-Nitro-3-butylbenzo[1,2,3]triazin-4(3H)-one (10b). Compound **9b** (3 g, 12.8 mmol), HCl solution (30%, 5 mL) and sodium nitrite (1.13 g, 16.6 mmol) were used to prepare white powder; yield: (2.75 g, 91%); m.p. 217–218 °C. FT-IR (ν -cm⁻¹): 1341 (NO₂), 1535 (NO₂), 1591 (C=O), 2962 (CH₂).

3.1.5. General Procedure for the Synthesis of 6-Amino-3-alkylbenzo[1,2,3]triazin-4(3H)-one (11a–11b)

Compound **10a–10b** (0.967 mmol), iron powder (2.42 g, 10 mmol) and HCl (30%, 5 mL) solution were taken in water (10 mL). Reaction mixture was stirred for two hours at 60 °C. Afterwards, the reaction mixture was filtered and the filtrate was cooled until crystals of product appeared. It was then recrystallized with chloroform.

6-Amino-3-propylbenzo[1,2,3]triazin-4(3H)-one (11a). Compound **10a** (0.15 g, 0.967 mmol), iron powder (2.42 g, 10 mmol) and HCl (30%, 5 mL) solution were used to obtain transparent crystals; yield: (0.11 g, 80%); m.p. 185–186 °C. FT-IR (ν -cm⁻¹): 1255 (C-N), 1638 (C=O), 2957 (CH₂), 3435 (NH₂); ¹H-NMR: (CDCl₃, 500 MHz): δ_{H} 0.891 (t, J = 7.5 Hz, 3H, CH₃), 1.73–1.81 (m, 2H, CH₂), 4.22 (t, J = 7.2 Hz, 2H, CH₂), 6.56 (s, 2H, NH₂), 7.16 (dd, J = 10.0, 2.5 Hz, 1H, ArH), 7.19 (d, J = 3.0 Hz, 1H, ArH), 7.81 (d, J = 8.5 Hz, 1H, ArH). ¹³C-NMR: (DMSO-d₆, 126 MHz): δ_{C} 11.5 (C, NCH₂CH₂CH₃), 22.3 (C, NCH₂CH₂CH₃), 50.6 (C, NCH₂CH₂CH₃), 103.4 (CH, C-5), 121.9 (CH, C-7), 122.3 (C, C-4a), 130.4 (CH, C-8), 136.2 (C, C-8a), 153.6 (C, C-6), 155.6 (CO, C-4).

6-Amino-3-butylbenzo[1,2,3]triazin-4(3H)-one (11b). Compound **10b** (0.24 g, 0.967 mmol), iron powder (2.42 g, 10 mmol) and HCl (30%, 5 mL) solution were used to prepare transparent crystals; yield: (0.18 g, 72%); m.p. 191–192 °C. FT-IR (ν -cm⁻¹): 1256 (C-N), 1693 (C=O), 2916 (CH₂), 3435 (NH₂); ¹H-NMR: (CDCl₃, 500 MHz): δ_{H} 0.85 (t, J = 7.3 Hz, 3H, CH₃), 1.25–1.28 (m, 2H, CH₂), 1.66–1.71 (m, 2H, CH₂), 4.22 (t, J = 7.2 Hz, 2H, CH₂), 6.55 (s, 2H, NH₂), 7.12 (d, J = 2.4 Hz, 1H, ArH), 7.15 (dd, J = 8.8, 2.5 Hz, 1H, ArH), 7.78 (d,

$J = 8.8$ Hz, 1H, Ar-H). ^{13}C -NMR: (DMSO- d_6 , 126 MHz): δ_{C} 14.0 (C, $\text{NCH}_2\text{CH}_2\text{CH}_2\text{CH}_3$), 19.8 (C, $\text{NCH}_2\text{CH}_2\text{CH}_2\text{CH}_3$), 31.0 (C, $\text{NCH}_2\text{CH}_2\text{CH}_2\text{CH}_3$), 48.7 (C, $\text{NCH}_2\text{CH}_2\text{CH}_2\text{CH}_3$), 103.4 (CH, C-5), 121.9 (CH, C-7), 122.3 (C, C-4a), 130.4 (CH, C-8), 136.2 (C, C-8a), 153.6 (C, C-6), 155.6 (CO, C-4).

3.1.6. General Procedure for the Synthesis of N-(4-Oxo-3-propyl/butyl-3,4-dihydrobenzo[1,2,3]triazin-6-yl)benzenesulfonamides (12a-12f)

Compound **11a/11b** (0.1 g, 0.49 mmol), benzene sulfonyl chloride (0.49 mmol) and pyridine (10 mL) were taken in a 50 mL round bottom flask and refluxed for 5 h. Then, the pyridine was evaporated under reduced pressure and the mixture was cooled to room temperature. A few drops of dilute HCl were added to ice-cold water (100 mL) until the pH reached 3, and the temperature was maintained at 5 °C. Further, the reaction mixture was poured off into acidified water. Precipitates appearing in the solution were filtered, dried and recrystallized from methanol. The physicochemical properties of all synthesized compounds are given in Table 3.

Table 3. Physicochemical properties of all synthesized compounds 7–12f.

Entry	Compound	Molecular Formula	Molecular Weight	Physical Appearance	% Yield	m.p. (°C)	Solubility
1.	7	$\text{C}_8\text{H}_5\text{NO}_3$	163.13	Light yellow powder	85%	230–232	Ethanol, DMSO
2.	8	$\text{C}_8\text{H}_4\text{N}_2\text{O}_5$	208.13	Yellow powder	62%	219–221	Ethanol, DMSO
3.	9a	$\text{C}_{10}\text{H}_{13}\text{N}_3\text{O}_3$	223.23	Mustard powder	60%	195–197	Ethanol, DMSO
4.	9b	$\text{C}_{11}\text{H}_{15}\text{N}_3\text{O}_3$	237.26	Mustard powder	58%	197–199	Ethanol, DMSO
5.	10a	$\text{C}_{10}\text{H}_{10}\text{N}_4\text{O}_3$	234.21	Light yellow powder	92%	215–217	Ethanol, DMSO
6.	10b	$\text{C}_{11}\text{H}_{12}\text{N}_4\text{O}_3$	248.24	White powder	91%	217–218	Ethanol, DMSO
7.	11a	$\text{C}_{10}\text{H}_{12}\text{N}_4\text{O}$	204.23	Transparent crystals	80%	185–186	Methanol, DMSO
8.	11b	$\text{C}_{11}\text{H}_{14}\text{N}_4\text{O}$	218.26	Transparent crystals	72%	191–192	Methanol, DMSO
9.	12a	$\text{C}_{16}\text{H}_{16}\text{N}_4\text{O}_3\text{S}$	344.39	Brown powder	82%	171–173	Ethanol, DMSO
10.	12b	$\text{C}_{17}\text{H}_{18}\text{N}_4\text{O}_4\text{S}$	374.41	Brown powder	75%	175–177	Ethanol, DMSO
11.	12c	$\text{C}_{16}\text{H}_{15}\text{ClN}_4\text{O}_3\text{S}$	378.83	Brown powder	68%	169–171	Ethanol, DMSO
12.	12d	$\text{C}_{16}\text{H}_{15}\text{BrN}_4\text{O}_3\text{S}$	423.28	Brown powder	78%	171–179	Ethanol, DMSO
13.	12e	$\text{C}_{16}\text{H}_{15}\text{N}_5\text{O}_5\text{S}$	389.39	Brown powder	71%	167–169	Ethanol, DMSO
14.	12f	$\text{C}_{17}\text{H}_{17}\text{N}_5\text{O}_5\text{S}$	403.41	Brown powder	62%	179–181	Ethanol, DMSO

N-(4-Oxo-3-propyl-3,4-dihydrobenzo[1,2,3]triazin-6-yl)benzenesulfonamide (**12a**). Benzene-sulfonyl chloride (0.15 g, 0.49 mmol) and compound **11a** (0.1 g, 0.49 mmol) were used to prepare brown powder; yield: (0.18 g, 82%); m.p. 171–173 °C. FT-IR ($\nu\text{-cm}^{-1}$): 1167 (S=O), 1331 (S=O), 1659 (C=O), 2964 (CH_2), 3185 (N-H); ^1H -NMR: (CDCl_3 , 300 MHz): δ_{H} 1.01 (t,

$J = 7.5$ Hz, 3H, CH₃), 1.90–1.97 (m, 2H, CH₂), 4.82 (t, $J = 7.2$ Hz, 2H, CH₂), 7.44 (t, $J = 7.3$ Hz, 2H, ArH), 7.52 (t, $J = 7.2$ Hz, 1H, ArH), 7.90 (d, $J = 7.5$ Hz, 2H, ArH), 7.93–8.12 (m, 3H, ArH), 8.59 (s, 1H, NH). ¹³C-NMR: (DMSO-d₆, 126 MHz): δ_C 11.5 (C, NCH₂CH₂CH₃), 22.1 (C, NCH₂CH₂CH₃), 51.2 (C, NCH₂CH₂CH₃), 111.3 (CH, C-5), 120.9 (CH, C-7), 126.1 (C, C-4a), 127.2 (2CH, C-2', C-6'), 130.2 (2CH, C-3', C-5'), 130.5 (CH, C-8), 134.1 (CH, C-4'), 139.4 (C, C-6), 140.4 (C, C-8a), 142.1 (C, C-1'), 155.0 (CO, C-4).

4-Methoxy-N-(4-oxo-3-propyl-3,4-dihydrobenzo[1,2,3]triazin-6-yl)benzenesulfonamide (12b). 4-Methoxybenzenesulfonyl chloride (0.11 g, 0.49 mmol) and compound **11a** (0.1 g, 0.49 mmol) were used to synthesize brown powder; yield: (0.13 g, 75%); m.p. 175–177 °C. FT-IR (v-cm⁻¹): 1158 (S=O), 1333 (S=O), 1664 (C=O), 2964 (CH₂), 3222 (N-H); ¹H-NMR: (DMSO-d₆, 500 MHz): δ_H 0.84 (t, $J = 7.5$ Hz, 3H, CH₃), 1.71–1.76 (m, 2H, CH₂), 3.73 (s, 3H, OCH₃), 4.22 (t, $J = 7.3$ Hz, 2H, CH₂), 7.05 (d, $J = 9.0$ Hz, 2H, ArH), 7.69–7.81 (m, 4H, ArH), 8.06 (d, $J = 2.1$ Hz, 1H, ArH), 11.22 (s, 1H, NH). ¹³C-NMR: (DMSO-d₆, 126 MHz): δ_C 11.5 (C, NCH₂CH₂CH₃), 22.1 (C, NCH₂CH₂CH₃), 51.2 (C, NCH₂CH₂CH₃), 56.2 (C, OCH₃), 111.0 (CH, C-5), 115.3 (2CH, C-3', C-5'), 120.9 (CH, C-7), 125.9 (C, C-4a), 129.5 (2CH, C-2', C-6), 130.4 (CH, C-8), 130.9 (C, C-1'), 140.3 (C, C-6), 142.4 (C, C-8a), 155.0 (CO, C-4), 163.4 (C, C-4').

4-Chloro-N-(4-oxo-3-propyl-3,4-dihydrobenzo[1,2,3]triazin-6-yl)benzenesulfonamide (12c). 4-Chlorobenzenesulfonyl chloride (0.1 g, 0.49 mmol) and compound **11a** (0.1 g, 0.49 mmol) were used to prepare brown powder; yield: (0.13 g, 68%); m.p. 169–171 °C. FT-IR (v-cm⁻¹): 1161 (S=O), 1333 (S=O), 1656 (C=O), 2961 (CH₂), 3193 (NH); ¹H-NMR: (DMSO-d₆, 500 MHz): δ_H 0.84 (t, $J = 7.2$ Hz, 3H, CH₃), 1.74–1.77 (m, 2H, CH₂), 4.22 (t, $J = 7.1$ Hz, 2H, CH₂), 7.70–7.78 (m, 5H, ArH), 7.81 (d, $J = 1.5$ Hz, 1H, ArH), 8.08 (d, $J = 8.5$ Hz, 1H, ArH), 11.40 (s, 1H, NH). ¹³C-NMR: (DMSO-d₆, 126 MHz): δ_C 11.5 (C, NCH₂CH₂CH₃), 22.1 (C, NCH₂CH₂CH₃), 51.2 (C, NCH₂CH₂CH₃), 111.7 (CH, C-5), 121.0 (CH, C-7), 126.3 (C, C-4a), 128.1 (CH, C-8), 129.2 (2CH, C-2', C-6'), 130.5 (C, C-6), 133.3 (2CH, C-3', C-5'), 138.7 (C, C-4'), 140.6 (C, C-1'), 141.8 (C, C-8a), 155.0 (CO, C-4).

4-Bromo-N-(4-oxo-3-propyl-3,4-dihydrobenzo[1,2,3]triazin-6-yl)benzenesulfonamide (12d). 4-Bromobenzenesulfonyl chloride (0.13 g, 0.49 mmol) and compound **11a** (0.1 g, 0.49 mmol) were used to obtain brown powder; yield: (0.14 g, 78%); m.p. 177–179 °C. FT-IR (v-cm⁻¹): 1164 (S=O), 1332 (S=O), 1657 (C=O), 2972 (CH₂), 3181 (N-H); ¹H-NMR: (DMSO-d₆, 500 MHz) δ_H : 0.85 (t, $J = 7.4$ Hz, 3H, CH₃), 1.70–1.78 (m, 2H, CH₂), 4.23 (t, $J = 7.4$ Hz, 2H, CH₂), 7.62 (d, $J = 8.0$ Hz, 2H, ArH), 7.70 (dd, $J = 8.8$ Hz, 2.5 Hz, 1H, ArH), 7.81–7.83 (m, 3H, ArH), 8.08 (d, $J = 8.8$ Hz, 1H, ArH), 11.38 (s, 1H, NH). ¹³C-NMR: (CDCl₃, 100 MHz): δ_C 11.7 (C, NCH₂CH₂CH₃), 22.2 (C, NCH₂CH₂CH₃), 51.0 (C, NCH₂CH₂CH₃), 111.7 (CH, C-5), 120.0 (CH, C-7), 126.3 (C, C-4a), 128.1 (CH, C-8), 129.2 (2CH, C-2', C-6'), 130.5 (2CH, C-3', C-5'), 133.3 (C, C-6), 138.7 (C, C-4'), 140.6 (C, C-1'), 141.8 (C, C-8a), 158.0 (CO, C-4).

4-Nitro-N-(4-oxo-3-propyl-3,4-dihydrobenzo[1,2,3]triazin-6-yl)benzenesulfonamide (12e). 4-Nitrobenzenesulfonyl chloride (0.11 g, 0.49 mmol) and compound **11a** (0.1 g, 0.49 mmol) were used to obtain brown powder; yield: (0.14 g, 71%); m.p. 167–169 °C. FT-IR (v-cm⁻¹): 1161 (S=O), 1357 (S=O), 1696 (C=O), 2932 (CH₂), 3210 (NH); ¹H-NMR: (DMSO-d₆, 500 MHz) δ_H : 0.85 (t, $J = 7.3$ Hz, 3H, CH₃), 1.72–1.76 (m, 2H, CH₂), 4.23 (t, $J = 7.0$ Hz, 2H, CH₂), 7.70–7.78 (m, 5H, ArH), 7.81 (d, $J = 1.5$ Hz, 1H, ArH), 8.08 (d, $J = 8.8$ Hz, 1H, ArH), 11.36 (s, 1H, NH). ¹³C-NMR: (DMSO-d₆, 126 MHz): δ_C 11.5 (C, NCH₂CH₂CH₃), 22.1 (C, NCH₂CH₂CH₃), 51.2 (C, NCH₂CH₂CH₃), 111.3 (CH, C-5), 120.9 (CH, C-7), 126.1 (C, C-4a), 127.2 (2CH, C-3', C-5'), 130.2 (2CH, C-2', C-6'), 130.5 (CH, C-8), 134.1 (C, C-6), 139.4 (C, C-8a), 140.4 (C, C-1'), 142.1 (C, C-4'), 155.0 (CO, C-4).

4-Nitro-N-(4-oxo-3-butyl-3,4-dihydrobenzo[1,2,3]triazin-6-yl)benzenesulfonamide (12f). 4-Nitrobenzenesulfonyl chloride (0.12 g, 0.49 mmol) and compound **11b** (0.1 g, 0.49 mmol) were used to obtain brown powder; yield: (0.06 g, 62%); m.p. 179–181 °C. FT-IR (v-cm⁻¹): 1189 (S=O), 1380 (S=O), 1597 (C=O), 2919 (CH₂), 3221 (NH); ¹H-NMR: (DMSO-d₆, 500 MHz) δ_H : 0.84 (t, $J = 7.4$ Hz, 3H, CH₃), 1.66–1.79 (m, 2H, CH₂), 2.20–2.24 (m, 4H, CH₂), 4.23–4.27 (m, 2H, CH₂), 7.34 (m, 2H, ArH), 7.71–7.81 (m, 4H, ArH), 8.04 (s, 1H, ArH), 11.32 (s, 1H, NH). ¹³C-NMR: (CDCl₃, 100 MHz): δ_C 11.5 (C, NCH₂CH₂CH₂CH₃), 21.5 (C, NCH₂CH₂CH₂CH₃), 22.1 (C, NCH₂CH₂CH₂CH₃), 51.2 (C, CH₂CH₂CH₂CH₃), 111.2 (2CH, C-5,

C-7), 120.9 (CH, C-4a), 126.0 (2C, C-3', C-5'), 127.2 (CH, C-8), 130.6 (2C, C-2', C-6'), 134.6 (C, C-6), 140.4 (C, C-8a), 142.3 (C, C-1'), 144.7 (C, C-4'), 155.0 (CO-C-4).

3.2. Procedure of Alpha-Glucosidase Inhibition Assay

Alpha-glucosidase inhibition activity was carried out by the Pierre *et al.* method with slight modifications, and alpha-Glucosidase (Cat No. 5003-1KU Type I) from *Saccharomyces cerevisiae* was utilized for the experimental protocol due to its resemblances to the structure and function of yeast/mammalian enzyme. For test, saline phosphate buffer (70 μ L, 50 mM with pH 6.8), alpha-glucosidase enzyme (10 μ L, 0.0234 units) and test compound (10 μ L, 0.5 mM) were taken in test tubes and incubated for 10 min at 37 °C. Absorbance of these prepared samples was recorded at 400 nm. 10 μ L *p*-nitrophenyl-alpha-D-glucopyranoside (0.5 mM, 'substrate', code No. N1377 from Sigma) was used to initiate the reaction and test tubes were allowed to stand for 30 min. Then, the variation in concentration of free substrate was noted by the change in absorbance. The enzyme percentage inhibition was estimated by the following formula and IC₅₀ values were calculated by 'EZ-Fit enzyme kinetics software.

$$\% \text{ Inhibition} = [(Abs. \text{ of test} - Abs. \text{ of control}) / Abs. \text{ of control}] \times 100$$

4. Conclusions

A series of 1,2,3-benzotriazin-4(3*H*)-one based sulfonamides was designed, synthesized and discovered to be effective alpha-glucosidase inhibitors. Among all other derivatives, compound **12e** (IC₅₀ 32.37 \pm 0.15 μ M) was found to be a better inhibitor as compared to the standard drug acarbose (IC₅₀ 37.38 \pm 0.12 μ M). Moreover, the inhibition potential of hybrid **12f** (IC₅₀ 37.75 \pm 0.11 μ M) was observed to be comparable to the reference drug. The enzyme inhibition mechanism was unlocked by molecular docking studies and significant interactions between the leading ligands and the targeted receptor were explored. In DFT, frontier molecular orbital analysis and molecular electrostatic potential studies were employed to understand various electronic parameters of all synthesized compounds. The least energy gap (E_{gap}) value between HOMO and LUMO depicted the reactive nature of **12e** and **12f**. In addition, the higher electrophilicity value of these compounds also acknowledged their interactive nature towards biomolecules. The electrophilic and nucleophilic sites of all synthesized compounds were shown by MEP studies. Hence, the *in vitro* alpha-glucosidase inhibitory results were in good agreement with the outcomes of molecular docking and the performed DFT calculations.

Supplementary Materials: The following supporting information can be downloaded at: <https://www.mdpi.com/article/10.3390/molecules27206783/s1>, Figure S1: FTIR spectrum of 7; Figure S2: FTIR spectrum of 8; Figure S3: FTIR spectrum of 9a; Figure S4: FTIR spectrum of 9b; Figure S5: FTIR spectrum of 10a; Figure S6: FTIR spectrum of 10b; Figure S7: FTIR spectrum of 11a; Figure S8: 1H NMR spectrum of 11a; Figure S9: 13C NMR spectrum of 11a; Figure S10: FTIR spectrum of 11b; Figure S11: 1H-NMR spectrum of 11b; Figure S12: 13C-NMR spectrum of 11b; Figure S13: FTIR spectrum of 12a; Figure S14: 1H-NMR spectrum of 12a; Figure S15: 13C-NMR spectrum of 12a; Figure S16: FTIR spectrum of 12b; Figure S17: 1H-NMR spectrum of 12b; Figure S18: 13C-NMR spectrum of 12b; Figure S19: FTIR spectrum of 12c; Figure S20: 1H-NMR spectrum of 12c; Figure S21: 13C-NMR spectrum of 12c; Figure S22: FTIR spectrum of 12d; Figure S23: 1H-NMR spectrum of 12d; Figure S24: 13C-NMR spectrum of 12d; Figure S25: FTIR spectrum of 12e; Figure S26: 1H-NMR spectrum of 12e; Figure S27: 13C-NMR spectrum of 12e; Figure S28: FTIR spectrum of 12f; Figure S29: 1H-NMR spectrum of 12f; Figure S30: 13C-NMR spectrum of 12f; Table S1: Binding energies of the docked compounds 7a-f inside the active sites of α -glucosidase.

Author Contributions: Conceptualization, M.A.M. and M.A.A.; methodology, Z.K. and H.A.A.; synthesis, Z.K. and H.A.A.; characterization, S.S.S., K.K. and M.A.E.; enzyme inhibition studies, H.A.A. and M.A.M.; manuscript writing, review, and editing, Z.K. and M.A.K.; supervision, M.M.A. All authors have read and agreed to the published version of the manuscript.

Funding: Princess Nourah bint Abdulrahman University Researchers Supporting Project number (PNURSP2022R186), Princess Nourah bint Abdulrahman University, Riyadh, Saudi Arabia.

Institutional Review Board Statement: Not applicable.

Informed Consent Statement: Not applicable.

Data Availability Statement: The data presented in this study are available in the Supplementary Materials. Samples of the compounds are available from the authors.

Acknowledgments: This work was supported by Princess Nourah bint Abdulrahman University researcher supporting project number (PNURSP2022R186), Princess Nourah bint Abdulrahman University, Riyadh, Saudi Arabia.

Conflicts of Interest: The authors declare no conflict of interest.

References

1. Saddique, F.; Aslam, S.; Ahmad, M.; Ashfaq, U.; Muddassar, M.; Sultan, S.; Taj, S.; Hussain, M.; Lee, D.S.; Zaki, M. Synthesis and α -Glucosidase Inhibition Activity of 2-[3-(Benzoyl/4-bromobenzoyl)-4-hydroxy-1,1-dioxido-2H-benzo[e][1,2]thiazin-2-yl]-N-arylacetamides: An In Silico and Biochemical Approach. *Molecules* **2021**, *26*, 3043. [[CrossRef](#)]
2. Zhang, X.; Zheng, Y.-Y.; Hu, C.-M.; Wu, X.-Z.; Lin, J.; Xiong, Z.; Zhang, K.; Xu, X.-T. Synthesis and biological evaluation of coumarin derivatives containing oxime ester as α -glucosidase inhibitors. *Arab. J. Chem.* **2022**, *15*, 104072. [[CrossRef](#)]
3. Dean, L.; McEntyre, J. Introduction to diabetes. In *The Genetic Landscape of Diabetes*; National Center for Biotechnology Information: Bethesda, MD, USA, 2004.
4. Kasturi, S.P.; Surarapu, S.; Uppalanchi, S.; Dwivedi, S.; Yogeewari, P.; Sigalapalli, D.K.; Bathini, N.B.; Ethiraj, K.S.; Anireddy, J.S. Synthesis, molecular modeling and evaluation of α -glucosidase inhibition activity of 3,4-dihydroxy piperidines. *Eur. J. Med. Chem.* **2018**, *150*, 39–52. [[CrossRef](#)]
5. Ibrar, A.; Zaib, S.; Khan, I.; Shafique, Z.; Saeed, A.; Iqbal, J. New prospects for the development of selective inhibitors of α -glucosidase based on coumarin-iminothiazolidinone hybrids: Synthesis, *in-vitro* biological screening and molecular docking analysis. *J. Taiwan Inst. Chem. Eng.* **2017**, *81*, 119–133. [[CrossRef](#)]
6. Temneanu, O.; Trandafir, L.; Purcarea, M.R. Type 2 diabetes mellitus in children and adolescents: A relatively new clinical problem within pediatric practice. *J. Med. Life* **2016**, *9*, 235–239. [[PubMed](#)]
7. Hu, F.B.; Manson, J.E.; Stampfer, M.J.; Colditz, G.; Liu, S.; Solomon, C.G.; Willett, W.C. Diet, Lifestyle, and the Risk of Type 2 Diabetes Mellitus in Women. *N. Engl. J. Med.* **2001**, *345*, 790–797. [[CrossRef](#)] [[PubMed](#)]
8. Ogurtsova, K.; Guariguata, L.; Barengo, N.C.; Ruiz, P.L.-D.; Sacre, J.W.; Karuranga, S.; Sun, H.; Boyko, E.J.; Magliano, D.J. IDF diabetes Atlas: Global estimates of undiagnosed diabetes in adults for 2021. *Diabetes Res. Clin. Pract.* **2022**, *183*, 109118. [[CrossRef](#)]
9. Abdullah, M.A.; Lee, Y.-R.; Mastuki, S.N.; Leong, S.W.; Ibrahim, W.N.W.; Latif, M.A.M.; Ramli, A.N.M.; Aluwi, M.F.F.M.; Faudzi, S.M.M.; Kim, C.-H. Development of diarylpentadienone analogues as alpha-glucosidase inhibitor: Synthesis, *in vitro* biological and *in vivo* toxicity evaluations, and molecular docking analysis. *Bioorg. Chem.* **2020**, *104*, 104277. [[CrossRef](#)] [[PubMed](#)]
10. Fallah, Z.; Tajbakhsh, M.; Alikhani, M.; Larijani, B.; Faramarzi, M.A.; Hamedifar, H.; Mohammadi-Khanaposhtani, M.; Mahdavi, M. A review on synthesis, mechanism of action, and structure-activity relationships of 1,2,3-triazole-based α -glucosidase inhibitors as promising anti-diabetic agents. *J. Mol. Struct.* **2022**, *1255*, 132469. [[CrossRef](#)]
11. Kazmi, M.; Zaib, S.; Amjad, S.T.; Khan, I.; Ibrar, A.; Saeed, A.; Iqbal, J. Exploration of aroyl/heteroaroyl iminothiazolines featuring 2,4,5-trichlorophenyl moiety as a new class of potent, selective, and *in vitro* efficacious glucosidase inhibitors. *Bioorg. Chem.* **2017**, *74*, 134–144. [[CrossRef](#)]
12. Karrouchi, K.; Fettach, S.; Tamer, Ö.; Avci, D.; Başoğlu, A.; Atalay, Y.; Ayaz, Z.; Radi, S.; Ghabbour, H.A.; Mabkhot, Y.N.; et al. Synthesis, crystal structure, spectroscopic characterization, α -glucosidase inhibition and computational studies of (E)-5-methyl-N'-(pyridin-2-ylmethylene)-1H-pyrazole-3-carbohydrazide. *J. Mol. Struct.* **2022**, *1248*, 131506. [[CrossRef](#)]
13. Kazmi, M.; Zaib, S.; Ibrar, A.; Amjad, S.T.; Shafique, Z.; Mehsud, S.; Saeed, A.; Iqbal, J.; Khan, I. A new entry into the portfolio of α -glucosidase inhibitors as potent therapeutics for type 2 diabetes: Design, bioevaluation and one-pot multi-component synthesis of diamine-bridged coumarinyl oxadiazole conjugates. *Bioorg. Chem.* **2018**, *77*, 190–202. [[CrossRef](#)] [[PubMed](#)]
14. Natori, Y.; Imahori, T.; Murakami, K.; Yoshimura, Y.; Nakagawa, S.; Kato, A.; Adachi, I.; Takahata, H. The synthesis and biological evaluation of 1-C-alkyl-l-arabinoiminofuranoses, a novel class of α -glucosidase inhibitors. *Bioorg. Med. Chem. Lett.* **2011**, *21*, 738–741. [[CrossRef](#)] [[PubMed](#)]
15. Khalid, Z.; Shafqat, S.S.; Ahmad, H.A.; Rehman, H.M.; Munawar, M.A.; Ahmad, M.; Asiri, A.M.; Ashraf, M. Synthesis of 1,2,3-benzotriazin-4(3H)-one derivatives as α -glucosidase inhibitor and their *in-silico* study. *Med. Chem. Res.* **2022**, *31*, 819–831. [[CrossRef](#)]
16. Kim, H.-R.; Antonisamy, P.; Kim, Y.-S.; Lee, G.; Ham, H.-D.; Kwon, K.-B. Inhibitory effect of Amomum villosum water extracts on α -glucosidase activity. *Physiol. Mol. Plant Pathol.* **2022**, *117*, 101779. [[CrossRef](#)]

17. Khan, I.; Khan, A.; Halim, S.A.; Khan, M.; Zaib, S.; Al-Yahyaie, B.E.M.; Al-Harrasi, A.; Ibrar, A. Utilization of the common functional groups in bioactive molecules: Exploring dual inhibitory potential and computational analysis of keto esters against α -glucosidase and carbonic anhydrase-II enzymes. *Int. J. Biol. Macromol.* **2021**, *167*, 233–244. [[CrossRef](#)]
18. Karle, P.P.; Dhawale, S.C.; Mandade, R.J.; Navghare, V.V. Screening of Manilkara zapota (L) P. Royen stem bark ethanolic extract for *in vitro* α -glucosidase inhibition, preliminary antidiabetic effects, and improvement of diabetes and its complications in alloxan-induced diabetes in Wistar rats. *Bull. Natl. Res. Cent.* **2022**, *46*, 110. [[CrossRef](#)]
19. Ahmad, H.A.; Aslam, M.; Gul, S.; Mehmood, T.; Munawar, M.A. In vivo Anti Inflammation Studies of Novel 1, 2, 5 Oxadiazole Sulfonamide Hybrids. *Pak. J. Zool* **2021**, *54*, 1001–1500. [[CrossRef](#)]
20. Gulçin, İ.; Taslimi, P. Sulfonamide inhibitors: A patent review 2013–present. *Expert Opin. Ther. Pat.* **2018**, *28*, 541–549. [[CrossRef](#)]
21. Wang, G.; Chen, M.; Wang, J.; Peng, Y.; Li, L.; Xie, Z.; Deng, B.; Chen, S.; Li, W. Synthesis, biological evaluation and molecular docking studies of chromone hydrazone derivatives as α -glucosidase inhibitors. *Bioorg. Med. Chem. Lett.* **2017**, *27*, 2957–2961. [[CrossRef](#)]
22. Taha, M.; Alrashedy, A.S.; Almandil, N.B.; Iqbal, N.; Anouar, E.H.; Nawaz, M.; Uddin, N.; Chigurupati, S.; Wadood, A.; Rahim, F.; et al. Synthesis of indole derivatives as diabetics II inhibitors and enzymatic kinetics study of α -glucosidase and α -amylase along with their in-silico study. *Int. J. Biol. Macromol.* **2021**, *190*, 301–318. [[CrossRef](#)] [[PubMed](#)]
23. Taha, M.; Imran, S.; Salahuddin, M.; Iqbal, N.; Rahim, F.; Uddin, N.; Shehzad, A.; Farooq, R.K.; Alomari, M.; Khan, K.M. Evaluation and docking of indole sulfonamide as a potent inhibitor of α -glucosidase enzyme in streptozotocin –induced diabetic albino wistar rats. *Bioorg. Chem.* **2021**, *110*, 104808. [[CrossRef](#)] [[PubMed](#)]
24. Selim, Y.A.; El-Azim, M.H.M.A.; El-Farargy, A.F. Synthesis and Anti-inflammatory Activity of Some New 1,2,3-Benzotriazine Derivatives Using 2-(4-Oxo-6-phenylbenzo[d][1,2,3]triazin-3(4H)-yl)acetohydrazide as a Starting Material. *J. Heterocycl. Chem.* **2018**, *55*, 1756–1764. [[CrossRef](#)]
25. Fiorino, F.; Severino, B.; De Angelis, F.; Perissutti, E.; Frecentese, F.; Massarelli, P.; Bruni, G.; Collavoli, E.; Santagada, V.; Caliendo, G. Synthesis and *In-Vitro* Pharmacological Evaluation of New 5-HT_{1A} Receptor Ligands Containing a Benzotriazinone Nucleus. *Arch. Pharm.* **2008**, *341*, 20–27. [[CrossRef](#)] [[PubMed](#)]
26. Fadda, A.A.; Abdel-Latif, E.; Fekri, A.; Mostafa, A.R. Synthesis and Docking Studies of Some 1,2,3-Benzotriazine-4-one Derivatives as Potential Anticancer Agents. *J. Heterocycl. Chem.* **2019**, *56*, 804–814. [[CrossRef](#)]
27. Fiorino, F.; Caliendo, G.; Perissutti, E.; Severino, B.; Frecentese, F.; Preziosi, B.; Izzo, A.A.; Capasso, R.; Santagada, V. Synthesis by Microwave Irradiation and Antidiarrhoeal Activity of Benzotriazinone and Saccharine Derivatives. *Arch. Pharm.* **2005**, *338*, 548–555. [[CrossRef](#)] [[PubMed](#)]
28. Sorensen, E.S.; Macedo, A.B.; Resop, R.S.; Howard, J.N.; Nell, R.; Sarabia, I.; Newman, D.; Ren, Y.; Jones, R.B.; Planelles, V.; et al. Structure-Activity Relationship Analysis of Benzotriazine Analogues as HIV-1 Latency-Reversing Agents. *Antimicrob. Agents Chemother.* **2020**, *64*, e00888-20. [[CrossRef](#)] [[PubMed](#)]
29. Caliendo, G.; Fiorino, F.; Grieco, P.; Perissutti, E.; Santagada, V.; Meli, R.; Raso, G.M.; Zanesco, A.; De Nucci, G. Preparation and local anaesthetic activity of benzotriazinone and benzoyltriazole derivatives. *Eur. J. Med. Chem.* **1999**, *34*, 1043–1051. [[CrossRef](#)]
30. Yan, Y.-C.; Wu, W.; Huang, G.-Y.; Yang, W.-C.; Chen, Q.; Qu, R.-Y.; Lin, H.-Y.; Yang, G.-F. Pharmacophore-Oriented Discovery of Novel 1,2,3-Benzotriazine-4-one Derivatives as Potent 4-Hydroxyphenylpyruvate Dioxygenase Inhibitors. *J. Agric. Food Chem.* **2022**, *70*, 6644–6657. [[CrossRef](#)]
31. Khalid, Z.; Ahmad, H.A.; Munawar, M.A.; Khan, M.-U.; Gul, S. 1,2,3-Benzotriazin-4(3H)-ones: Synthesis, Reactions and Applications. *Heterocycles* **2017**, *94*, 3–54. [[CrossRef](#)]
32. Reddy, G.S.; Snehalatha, A.V.; Edwin, R.K.; Hossain, K.A.; Giliyaru, V.B.; Hariharapura, R.C.; Shenoy, G.G.; Misra, P.; Pal, M. Synthesis of 3-indolylmethyl substituted (pyrazolo/benzo)triazinone derivatives under Pd/Cu-catalysis: Identification of potent inhibitors of chorismate mutase (CM). *Bioorg. Chem.* **2019**, *91*, 103155. [[CrossRef](#)] [[PubMed](#)]
33. El Rayes, S.M.; Ali, I.A.I.; Fathalla, W.; Mahmoud, M.A.A. Synthesis and Biological Activities of Some New Benzotriazinone Derivatives Based on Molecular Docking; Promising HepG2 Liver Carcinoma Inhibitors. *ACS Omega* **2020**, *5*, 6781–6791. [[CrossRef](#)] [[PubMed](#)]
34. Moghimi, S.; Goli-Garmroodi, F.; Pilali, H.; Mahdavi, M.; Firoozpour, L.; Nadri, H.; Moradi, A.; Asadipour, A.; Shafiee, A.; Foroumadi, A. Synthesis and anti-acetylcholinesterase activity of benzotriazinone-triazole systems. *J. Chem. Sci.* **2016**, *128*, 1445–1449. [[CrossRef](#)]
35. Clark, R.H.; Wagner, E.C. Isatoic Anhydride. I. Reactions with Primary and Secondary Amines and with Some Amides¹. *J. Org. Chem.* **1944**, *9*, 55–67. [[CrossRef](#)]
36. Quadbeck-Seeger, H.-J.; Tonne, P. Production of Unsubstituted or Substituted Isatoic Anhydride. U.S. Patent 3,984,406, 5 October 1976.
37. Kanişkan, N.; Kökten, Ş.; Çelik, I. A new protocol for the synthesis of primary, secondary and tertiary anthranilamides utilizing N-(2-aminoaryllacyl)benzotriazoles. *Arkivoc* **2012**, *8*, 198–213. [[CrossRef](#)]
38. Ege, G.; Arnold, P.; Beisiegel, E.; Lehrer, I.; Suschitzky, H.; Price, D. Ringspaltung cyclischer Azoverbindungen, VII. 6-Fluor-sowie 6-Nitro-3-phenyl-3,4-dihydro-1,2,3-benzotriazin-4-on und deren Photolyse; nucleophile Substitution zur Erprobung der Fluor-Markierungsmethode von Suschitzky. *Eur. J. Org. Chem.* **1976**, *1976*, 946–968. [[CrossRef](#)]
39. Bashir, N.; Gilchrist, T.L. Formation of fused azetinones by photolysis and pyrolysis of triazinones. N-aminonaphth[2,3-b]azet-2(1H)-one and N-1-adamantylbenzazet-2(1H)-one. *J. Chem. Soc. Perkin Trans. 1* **1973**, 868–872. [[CrossRef](#)]

40. Ganesan, M.; Raja, K.K.; Murugesan, S.; Kumar, B.K.; Rajagopal, G.; Thirunavukkarasu, S. Synthesis, biological evaluation, molecular docking, molecular dynamics and DFT studies of quinoline-fluoroproline amide hybrids. *J. Mol. Struct.* **2020**, *1217*, 128360. [[CrossRef](#)]
41. Aslam, S.; Ali, H.S.; Ahmad, M.; Mansha, A.; Ali, N.; Khan, S.; Naqvi, S.A.R.; Khalid, Z.; Asim, S.; Parvez, M.; et al. A combined experimental and theoretical study of alkyl 2-(3-benzoyl-4-hydroxy-1,1-dioxido-2H-benzo[e][1,2]thiazin-2-yl)acetates: Synthesis, X-ray crystallography and DFT. *J. Mol. Struct.* **2022**, *1258*, 132671. [[CrossRef](#)]
42. Karrouchi, K.; Sert, Y.; Ansar, M.; Radi, S.; El Bali, B.; Imad, R.; Alam, A.; Irshad, R.; Wajid, S.; Altaf, M. Synthesis, α -Glucosidase Inhibition, Anticancer, DFT and Molecular Docking Investigations of Pyrazole Hydrazone Derivatives. *Polycycl. Aromat. Compd.* **2022**, 1–20. [[CrossRef](#)]
43. Alyar, S.; Şen, T.; Özmen, Ü.Ö.; Alyar, H.; Adem, S.; Şen, C. Synthesis, spectroscopic characterizations, enzyme inhibition, molecular docking study and DFT calculations of new Schiff bases of sulfa drugs. *J. Mol. Struct.* **2019**, *1185*, 416–424. [[CrossRef](#)]
44. Kharul, R.K.; Prajapati, P.N.; Thorave, A.A.; Shah, H.A.; Dhar, A.; Joshi, D.A.; Jain, M.R.; Patel, P.R.; Pancholi, S.S. Effective Synthesis of 1,5-Disubstituted 2,1-Benzisothiazol-3(1H)-ones. *Synth. Commun.* **2011**, *41*, 3265–3279. [[CrossRef](#)]